# Isotope Exchange at Equilibrium Indicates a Steady State Ordered Kinetic Mechanism for Human Sulfotransferase[†]

Eduard Tyapochkin,[‡] Paul F. Cook,*[,§] and Guangping Chen*[,‡]

*Department of Physiological Sciences, Center for Veterinary Health Sciences, Oklahoma State University, Stillwater, Oklahoma 74078, and Department of Chemistry and Biochemistry, University of Oklahoma, 620 Parrington Oval, Norman, Oklahoma 73019*

*Received June 27, 2008; Revised Manuscript Received August 12, 2008*

ABSTRACT: Cytosolic sulfotransferase (SULT)-catalyzed sulfation regulates biosignaling molecular biological activities and detoxifies hydroxyl-containing xenobiotics. The universal sulfuryl group donor for SULT-catalyzed sulfation is adenosine 3′-phosphate 5′-phosphosulfate (PAPS). The reaction products are a sulfated product and adenosine 3′,5′-diphosphate (PAP). Although the kinetics has been reported since the 1980s, SULT-catalyzed reaction mechanisms remain unclear. Human SULT1A1 catalyzes the sulfation of xenobiotic phenols and has very broad substrate specificity. It has been recognized as one of the most important phase II drug-metabolizing enzymes. Understanding the kinetic mechanism of this isoform is important in understanding drug metabolism and xenobiotic detoxification. In this report, we investigated the SULT1A1-catalyzed phenol sulfation mechanism. The SULT1A1-catalyzed reaction was brought to equilibrium by varying substrate (1-naphthol) and PAPS initial concentrations. Equilibrium constants were determined. Two isotopic exchanges at equilibrium ([$^{14}$C]1-naphthol $\rightleftharpoons$ [$^{14}$C]1-naphthyl sulfate and [$^{35}$S]PAPS $\rightleftharpoons$ [$^{35}$S]1-naphthyl sulfate) were conducted. First-order kinetics, observed for all the isotopic exchange reactions studied over the entire time scale that was monitored, indicates that the system was truly at equilibrium prior to addition of an isotopic pulse. Complete suppression of the $^{35}$S isotopic exchange rate was observed with an increase in the levels of 1-naphthol and 1-naphthyl sulfate in a constant ratio, while no suppression of the $^{14}$C exchange rate was observed with an increase in the levels of PAPS and PAP in a constant ratio. Data are consistent with a steady state ordered kinetic mechanism with PAPS and PAP binding to the free enzyme.

Sulfotransferases (SULTs)[1] catalyze the sulfation of hydroxyl-containing compounds as shown in Scheme 1 (*1*−*10*). The universal sulfuryl group donor for SULT-catalyzed sulfation is adenosine 3′-phosphate 5′-phosphosulfate (PAPS). The reaction products are a sulfated product and adenosine 3′,5′-diphosphate (PAP).

Studies of SULT catalytic mechanisms began in the early 1980s. However, the kinetic mechanism of sulfotransferases has not yet been clearly defined. Initial velocity studies of the rat aryl SULT (AST-IV) were consistent with either a rapid equilibrium random bi-bi mechanism with two dead-end product complexes or an ordered Theorell−Chance mechanism (*11*). On the other hand, similar studies of the kinetic mechanism of the human SULT1E1 were consistent with a random bi-bi mechanism with two dead-end complexes (*12*). Earlier kinetic studies of a bile salt SULT from human liver (*13*) and the insect SULT retinal dehydratase (*14*) also suggested a random kinetic mechanism.

Scheme 1: SULT-Catalyzed Reactions

$$\text{R-OH} + \text{PAPS} \overset{\text{SULTs}}{\rightleftharpoons} \text{R-OSO}_3\text{H} + \text{PAP}$$

Most of the SULTs that were studied appear to conform to a steady state ordered bi-bi kinetic mechanism in which PAPS is the leading substrate. Enzymes studied include STIII from female rats (*15*), human SULT1A3 (*16, 17*), rat tyrosyl protein SULT (*18, 19*), plant flavonol 3-SULT (*20*), and a SULT from *Klebsiella* K-36 (*21*). Careful studies of the mouse estrogen SULT, using initial rate studies, complemented by the crystal structure, structural modeling, and site-directed mutagenesis, were consistent with an ordered mechanism with PAPS binding first (*10, 22*−*30*). Studies of a SULT from rhesus monkey liver were also consistent with an ordered bi-bi mechanism for the sulfation of hepatotoxin glycolithocholate, but with the bile salt (not PAPS) as the leading substrate (*31*).

Studies of some bacterial SULTs, on the other hand, suggested a ping-pong bi-bi mechanism (*32*−*35*). A hybrid rapid-equilibrium random two-site ping-pong mechanism was proposed for the bacterial SULT, NodST, with the formation of a sulfated NodST intermediate (*32*). In this mechanism, PAPS and chitobiose bind independently and randomly at two different sites on NodST. The same group studied another bacterial SULT (Stf0) using mass spectrometry and concluded that it has a rapid-equilibrium random mechanism

[†] This work was supported in part by NIH Grant GM078606 (G.C.).

* To whom correspondence should be addressed. G.C.: e-mail, guangping.chen@okstate.edu; fax, (405) 744-1112. P.F.C.: e-mail, pcook@ou.edu; fax, (405) 325-7182.

[‡] Oklahoma State University.

[§] University of Oklahoma.

[1] Abbreviations: SULT, sulfotransferase; SULT1A1, simple phenol sulfotransferase; PAPS, adenosine 3′-phosphate 5′-phosphosulfate; PAP, adenosine 3′,5′-diphosphate; TLC, thin layer chromatography.

10.1021/bi801211t CCC: $40.75 
Published on Web 10/18/2008

(*36*). Studies of the bacterial arylsulfate SULT (ASST), which catalyzes the transfer of the sulfate group from a phenyl sulfate ester to the phenolic accepter, suggested a ping-pong mechanism. Site-directed mutagenesis suggested that Tyr123 was the residue in the ASST active site that accepts a sulfate for transfer to another phenolic substrate (*35*).

Human SULT1A1 is one of the major detoxifying enzymes for phenolic xenobiotics. It has very broad substrate specificity and high activity toward most phenolic compounds. It is also widely distributed in human tissues. The kinetic mechanism for human SULT1A1 has not been well studied. Isotope exchange at equilibrium is an excellent probe for the investigation of enzyme kinetic mechanisms (*37*−*39*). In this work, isotopic exchange at equilibrium is used to probe the kinetic mechanism of human SULT1A1. Our data suggested a steady state ordered kinetic mechanism.

## EXPERIMENTAL PROCEDURES

*Chemicals.* α-[$^{14}$C]1-Naphthol (55 mCi/mmol) was purchased from American Radiolabeled Chemicals, Inc. [$^{35}$S]Adenosine 3′-phosphate 5′-phosphosulfate (2.43 Ci/mmol) was purchased from PerkinElmer, Inc. (Boston, MA). 1-Naphthol and adenosine 3′,5′-diphosphate, sodium salt (PAP) were purchased from Sigma-Aldrich, while adenosine 3′-phosphate 5′-phosphosulfate, tetralithium salt (PAPS) was purchased from Calbiochem. 1-Naphthyl sulfate, potassium salt was purchased from MP Biomedicals, LLC.

Thin layer Partsil KC 18 F, silica Gel 60 chromatography plates, with a fluorescent indicator (20 cm × 20 cm, 200 μm) from Whatman Schleicher & Schuell, were purchased from Sigma-Aldrich. The plates were channeled using razor blades. A channel width of 1 cm was chosen with a groove width between channels of 2 mm. Deionized water was used in all the experiments. All other reagents and chemicals were of the highest available grade. Scintillation counting was carried out on a Beckman LS 6500 multipurpose scintillation counter.

*Enzyme.* SULT1A1 (7.5 mg/mL, maltose fusion protein) purified as described previously (*40*−*42*) was used in this study.

*Measurement of the Equilibrium Constant.* All the reactions were carried out in closed microcentrifuge tubes (0.5 mL) to prevent evaporation. The total reaction volume was 50 μL to bring the system to equilibrium quickly. SULT1A1 was added to the reaction mixture last to start the reaction. The time course for attaining equilibrium was first determined. For example, equilibrium was reached within 2 h for a solution containing 7.5 μg of SULT1A1 in 50 mM phosphate buffer (pH 6.2, 37 °C), where the initial concentrations of 1-naphthol and PAPS were 20 and 10 μM, respectively.

Different initial concentrations of PAPS and $^{14}$C-labeled 1-naphthol were incubated in 50 mM phosphate buffer (pH 6.2) at 37 °C, until equilibrium was attained. The reaction was stopped with 50 μL of TRIS base (0.25 M, pH 8.7). To separate $^{14}$C-labeled 1-naphthol from the product, $^{14}$C-labeled 1-naphthyl sulfate, 100 μL of chloroform was added to each Eppendorff tube. The mixture was vortexed for 30 s and centrifuged at 9000*g* for 5 min. 1-Naphthol is extracted into the chloroform phase, while 1-naphthyl sulfate remains in the aqueous phase. The chloroform phase was carefully separated from the aqueous phase using a microsyringe and then transferred into a scintillation vial containing 4 mL of scintillation cocktail (EcoLite) and counted. The syringe was rinsed with acetone twice between samples. The liquid−liquid extraction with chloroform was repeated twice. The aqueous phase containing product was transferred into a scintillation vial containing 4 mL of scintillation cocktail (EcoLite) and counted.

The $^{14}$C-labeled product was monitored until there was no longer any change with time. Once the system appeared to be at equilibrium, the same amount of SULT1A1 (7.5 μg) was added to the same reaction mixture to determine if any additional change in product was observed. If there was no change in product, $K_e$ was calculated according to eq 1.

$$K_e = \frac{[P]_e^{\,2}}{[S]_e([PAPS]_0 - [P]_e)} \quad (1)$$

where $[P]_e = [PAP]_e$ and $[S]_e = [S]_0 - [P]_e$. Equilibrium substrate and product concentrations were determined from calculated specific radioactivities for each experiment as discussed above.

Two types of controls were carried out. The first one made use of the same protocol as discussed above, but in the absence of SULT1A1, while the second one was conducted in the absence of PAPS and/or PAP. No significant difference was observed between the two types of control. The counts per minute of the controls was subtracted from those of the sample (aqueous phase only). All the controls and samples were carried out in triplicate; results are given as means ± the standard deviation (SD).

The method of equilibrium perturbation (*39*) was used to determine the equilibrium constant. The reaction mixture was equilibrated using $[[^{14}C]1\text{-naphthol}]_0$ and $[PAPS]_0$ values of 20 and 10 μM, respectively. Various concentrations of cold 1-naphthol and 1-naphthyl sulfate, such that the concentrations of the cold reactants were at least 1 order of magnitude greater than $[[^{14}C]1\text{-naphthol}]_0$, were added to the reaction mixture. The change in [$^{14}$C]1-naphthyl sulfate product concentration was monitored using a scintillation counter, as discussed above. The equilibrium position was established at the S/P ratio where no change in product occurs.

The equilibrium constant was also determined using [$^{35}$S]PAPS and 1-naphthol. The method was similar to the one described above. Termination of the reaction and separation of the labeled reactant and product were different. The reaction was stopped with 50 μL of methanol. Channeled silica gel TLC plates were used to separate [$^{35}$S]PAPS and [$^{35}$S]1-naphthyl sulfate. The reaction mixture (100 μL) was spotted onto a TLC plate using a micropipette in aliquots of 5 μL. The composition of the mobile phase for the TLC studies was determined experimentally by separating nonradioactive PAPS and product 1-naphthyl sulfate at 4 and 10 mM, respectively, and viewing the spots with 254 nm UV light. [$^{35}$S]PAPS and $^{35}$S-labeled product were best separated using an acetonitrile/methanol/acetic acid/water mixture (25:65:5:5). The TLC plates were developed in a closed glass chamber. After separation of [$^{35}$S]PAPS and $^{35}$S-labeled product, the dried TLC plates were subjected to autoradiography (24 h), and the radioactive spots were transferred into scintillation vials containing 4 mL of

scintillation cocktail (EcoLite) to determine the total amounts of [$^{35}$S]PAPS remaining and $^{35}$S-labeled product formed. Equilibrium concentrations and $K_e$ were calculated using an approach similar to the one described above.

*Isotope Exchange at Equilibrium.* The rates of isotopic exchange at equilibrium were determined by adding the radiolabeled reactant to the fully equilibrated reaction system containing SULT1A1. The total concentration of radiolabeled pulse was set at a concentration at least 100-fold lower than the cold reactant concentration. This ensured sufficient radioactivity for following the approach to isotopic equilibrium while allowing confirmation of the fact that a very limited change in the chemical equilibrium position occurs upon addition of the pulse. The formation of the radiolabeled product was monitored as a function of time until there was no more change. The reaction was then stopped with 50 $\mu$L of TRIS (0.25 M, pH 8.7). The liquid−liquid extraction protocol described above was used to separate labeled substrate and product. When [$^{35}$S]PAPS was used for these experiments, 50 $\mu$L of methanol was used to stop the reactions and the TLC method was used to separate radioactive PAPS and product as described above.

The rates of isotope exchange were calculated using eq 2 (*39*)

$$V_{ex} = \frac{AC \ln(1-f)}{(A+C)t[\text{enzyme}]} \quad (2)$$

where $V_{ex}$ is the initial velocity of isotopic exchange, $A$ and $C$ are the equilibrium amounts of the exchanging reactant and product, respectively (e.g., 1-naphthol and 1-naphthyl sulfate in micromoles), $t$ is the time required to reach the $f$ fraction of isotopic equilibrium in minutes, and $f$ is the fraction of isotopic equilibrium achieved at time $t$ $\{f = [(^{14}C)S]_t/[(^{14}C)S]_e = [(^{14}C)P]_t/[(^{14}C)P]_e\}$. Subscripts t and e indicate time-dependent and equilibrium values, respectively.

## RESULTS

*Equilibrium Constant.* The equilibrium constant, $K_e$, was determined independently by monitoring the approach to equilibrium beginning with varying $[PAPS]_0$ and $[1\text{-naphthol}]_0$ values or by measuring the perturbation from equilibrium. The $K_e$ was measured at different ratios of 1-naphthol to 1-naphthyl sulfate and PAPS to 1-naphthyl sulfate by monitoring the change in the concentration of the radiolabel as equilibrium was attained (Figure 1) (*39*). The S/P ratio that gives no change in product after addition of the cold reactants is the one that indicates the system is at equilibrium. The $K_e$ values measured are consistent using two different methods (Tables 1 and 2). The liquid−liquid extraction method is more accurate. The TLC method is intrinsically less accurate and gave errors larger than those obtained using liquid−liquid extraction with chloroform. The average value of $K_e$ used in subsequent experiments is 0.021 ± 0.004 (Table 1).

*[$^{14}$C]1-Naphthol−[$^{14}$C]1-Naphthyl Sulfate Isotope Exchange at Equilibrium.* The time required to achieve isotopic equilibrium for the exchange monitoring the appearance of [$^{14}$C]1-naphthyl sulfate is shown in Figure 2A; isotopic equilibrium was achieved within 2 h in all cases. When ln(1 − $f$) was plotted versus time in Figure 2B (where $f$ is the fraction of the equilibrium concentration of [$^{14}$C]1-naphthyl sulfate attained at time $t$), it clearly indicated a first-order reaction. All of the first-order plots were linear for all the isotopic exchange reactions studied over the entire time scale that was monitored. All the isotopic exchange rates were directly proportional to the enzyme concentration.

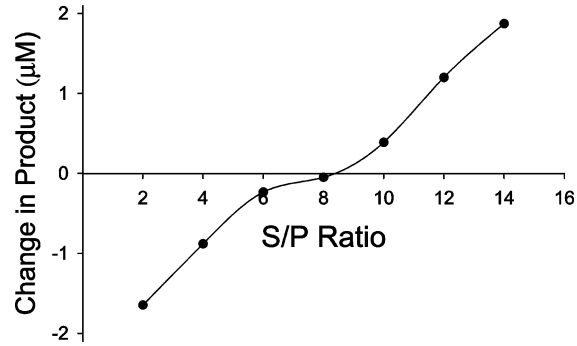


FIGURE 1: Determination of $K_e$ by varying the S/P ratio and measuring the change in the level of the radiolabeled reactant. The reaction mixture was equilibrated using a $[[^{14}C]1\text{-naphthol}]_0$ of 20 $\mu$M and a $[PAPS]_0$ of 10 $\mu$M and then adding S and P (cold) in different ratios to the reaction mixture. The change in product concentration was monitored using scintillation counting.

Table 1: $K_e$ Values Determined Using PAPS and [$^{14}$C]1-Naphthol

| $[PAPS]_0$ ($\mu$M) | $[[^{14}C]1\text{-naphthol}]_0$ ($\mu$M) | $K_e$ |
|---|---|---|
| 2 | 2 | 0.021 ± 0.004 |
| 2 | 4 | 0.019 ± 0.002 |
| 2 | 8 | 0.022 ± 0.003 |
| 10 | 10 | 0.023 ± 0.003 |
| 10 | 20 | 0.021 ± 0.003 |
| 10 | 50 | 0.023 ± 0.002 |
| 80 | 20 | 0.019 ± 0.002 |
| 80 | 40 | 0.024 ± 0.002 |
| 80 | 50 | 0.021 ± 0.003 |

Table 2: $K_e$ Values Determined Using [$^{35}$S]PAPS and 1-Naphthol

| $[[^{35}S]PAPS]_0$ ($\mu$M) | $[1\text{-naphthol}]_0$ ($\mu$M) | $K_e$ |
|---|---|---|
| 10 | 50 | 0.04 ± 0.01 |
| 10 | 100 | 0.031 ± 0.008 |

The exchange rate, $V_{ex}$, was calculated from the data in Figure 2 using eq 2. In panels A and B of Figure 2, the concentrations of PAPS and PAP were 20 and 4 $\mu$M, respectively, giving a $[PAPS]_0/[PAP]_0$ ratio of 5. Maintaining the PAPS/PAP ratio at 5, but increasing the concentrations of the two components, gave a family of curves similar to those shown in Figure 2. A plot of the calculated $V_{ex}$ versus the initial concentration of PAPS, with $[PAPS]_0/[PAP]_0$ maintained at 5, gave the hyperbolic plot shown in Figure 3. Fitting the data in Figure 3 to the Michaelis−Menten equation gave a $K_{PAPS}$ for the exchange reaction of 2.1 ± 0.5 $\mu$M, similar to the $K_{PAPS}$ value of 1 $\mu$M obtained for the chemical reaction, and a $V_{max}$ for the exchange reaction of 2.96 ± 0.03 $\mu$M min$^{-1}$ mg$^{-1}$. The hyperbolic nature of the $^{14}$C-labeled 1-naphthol to 1-naphthyl sulfate exchange rate indicates a lack of suppression of the exchange as a result of an increasing $[PAPS]_0/[PAP]_0$ ratio.

*[$^{35}$S]PAPS−[$^{35}$S]1-naphthyl Sulfate Isotope Exchange at Equilibrium.* Experiments similar to those described above were also conducted for the PAPS−1-naphthyl sulfate exchange with $^{35}$S as the label. The $[PAPS]_0/[PAP]_0$ concentration ratio was fixed at 5/1, and the $[S]_0/[P]_0$ (1-naphthol to 1-naphthyl sulfate) ratio was fixed at 10/1. The $V_{ex}$ was

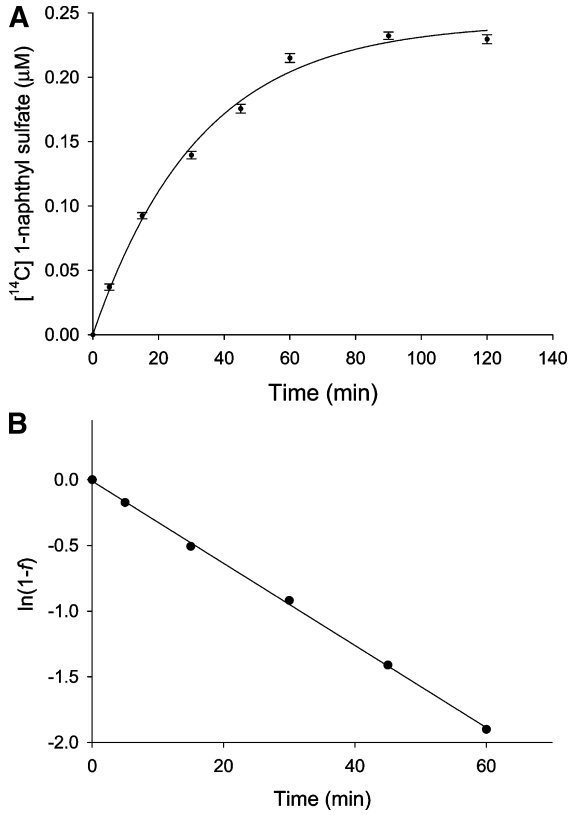


FIGURE 2: (A) Time course for the 1-naphthol to 1-naphthyl sulfate exchange reaction monitoring the appearance of [$^{14}$C]1-naphthyl sulfate. (B) First-order plot of the data in panel A as $\ln(1 - f)$ vs time. Concentrations of PAPS, PAP, 1-naphthol, and 1-naphthyl sulfate are 20, 4, 50, and 5 $\mu$M, respectively, consistent with the equilibrium constant. The concentration of the added [$^{14}$C]1-naphthol pulse is 0.5 $\mu$M. Each reaction mixture included 7.5 $\mu$g of SULT1A1 in 50 $\mu$L of phosphate buffer (final concentration of 50 mM, pH 6.2) at 37 °C. The curve fitting was done using Enzyme Kinetics Module 1.2 (SigmaPlot).

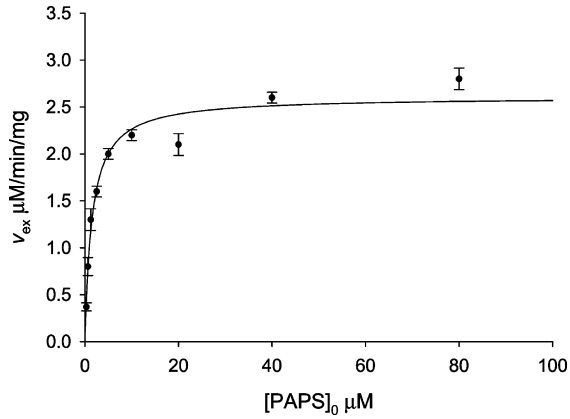


FIGURE 3: Initial rates of [$^{14}$C]S ⇌ [$^{14}$C]P isotopic exchange vs the $[PAPS]_0/[PAP]_0$ ratio. Concentrations of 1-naphthol and 1-naphthyl sulfate are 50 and 5 $\mu$M, respectively. The concentration of the added [$^{14}$C]1-naphthol pulse is 0.5 $\mu$M; 7.5 $\mu$g of SULT1A1 in 50 $\mu$L of phosphate buffer (final concentration of 50 mM, pH 6.2) was added at 37 °C. The curve fitting was done using Enzyme Kinetics Module 1.2 (SigmaPlot).

then measured as a function of the increasing concentration of 1-naphthol, with the $[S]_0/[P]_0$ ratio kept constant.

The maximal rate of the PAPS−1-naphthyl sulfate isotopic exchange was ~4-fold faster than that of the 1-naphthol−1-naphthyl sulfate isotopic exchange. Isotopic equilibrium was attained within ~30 min for the former compared to 1−2 h

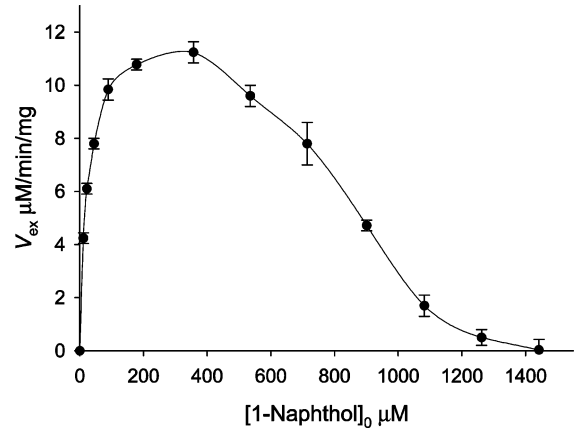


FIGURE 4: Rates of [$^{35}$S]PAPS ⇌ [$^{35}$S]P isotopic exchange vs $[S]_0/[P]_0$ ratio. Concentrations of PAPS and PAP were 10 and 2 $\mu$M, respectively. The concentration of the added [$^{35}$S]PAPS pulse is 0.05 $\mu$M; 7.5 $\mu$g of SULT1A1 in 50 $\mu$L of phosphate buffer (final concentration of 50 mM, pH 6.2) was added at 37 °C.

Scheme 2: Possible Mechanisms for SULT-Catalyzed Reactions

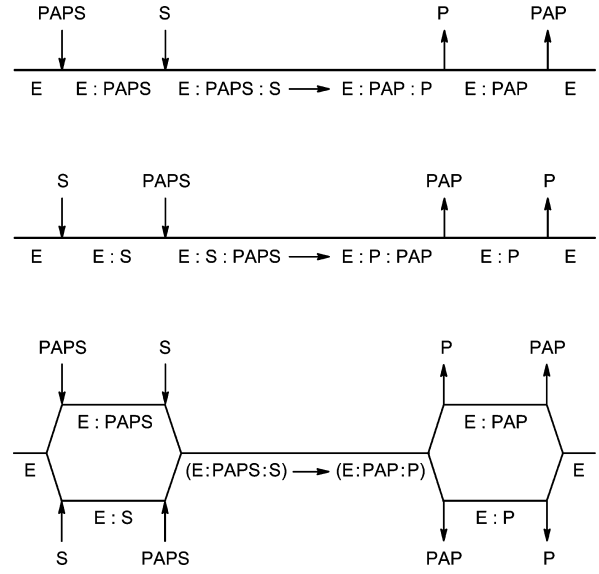


for the latter. All of the first-order plots were linear [similar to Figure 2B (data not shown)]. A plot of the $V_{ex}$ versus the concentration of 1-naphthol with 1-naphthol to 1-naphthyl sulfate maintained at a constant ratio exhibits substrate inhibition with a complete depression of $V_{ex}$ at high concentrations (Figure 4). When 1-naphthol concentrations reach >1.4 mM (140 $\mu$M 1-naphthyl sulfate), the exchange rate approaches zero.

## DISCUSSION

Three kinetic mechanisms have been postulated for SULT-catalyzed sulfation reactions, including a random mechanism, and one of two ordered mechanisms, that is, with PAPS and PAP binding to the free enzyme or with substrate and sulfated product binding to the free enzyme (Scheme 2). Although a ping-pong mechanism was postulated, it was observed only for bacterial SULTs.

In the case of a random mechanism (Scheme 2, bottom), all plots of $V_{ex}$ versus a reactant concentration at a constant ratio to product are usually hyperbolic but may exhibit partial suppression of the rate at high concentrations of the reactant/

product pair (*37*−*39*). In the case of a rapid equilibrium random kinetic mechanism, the maximum rates of all of the exchange reactions are equal, since all have the same rate-limiting step. However, in the case of an ordered mechanism, the exchange rate will be suppressed as the inner reactant/product pair ratio is increased to infinity (*37*−*39*). Thus, in the case of the ordered mechanism shown at the top of Scheme 2, increasing the 1-naphthol/1-naphthyl sulfate pair ratio will suppress the rate of exchange between PAPS and PAP, or PAPS and 1-naphthyl sulfate. For the ordered mechanism shown in the middle of Scheme 2, increasing the PAPS/PAP pair ratio will decrease the rate of exchange between 1-naphthol and 1-naphthyl sulfate, or PAPS and 1-naphthyl sulfate.

As shown in Figures 3 and 4, the rate of $^{14}C$ exchange between 1-naphthol and 1-naphthyl sulfate is not suppressed by an increase in the levels of PAPS and PAP in a constant ratio, but the rate of the $^{35}S$ exchange between PAPS and 1-naphthyl sulfate is completely suppressed at high concentrations of 1-naphthol and 1-naphthyl sulfate. When $V_{ex}$ was plotted versus 1/[1-naphthol] (not shown) for the data shown in Figure 4, $V_{ex}$ goes to zero when [1-naphthol] goes to infinity. This suggests that when substrate 1-naphthol binds to the active site first, human SULT1A1 will be inactive (PAPS unable to bind). The kinetic mechanism is basically strictly ordered with PAPS binding to the active site first. Product inhibition by PAPS is eliminated by the lack of observed substrate inhibition in the PAPS−PAP exchange experiments. The data are consistent with the ordered mechanism shown at the top of Scheme 2. The enzyme forms to which 1-naphthol and 1-naphthyl sulfate bind are E:PAPS and E:PAP. Therefore, increasing PAPS and PAP concentrations will increase the concentration of the two enzyme forms to which the exchanging pair binds, and increase the exchange rate. However, because PAPS binds to E and 1-naphthol binds to E:PAPS, increasing the 1-naphthol concentration to infinity will stop PAPS from binding to the enzyme and decrease the exchange rate. Thus, the mechanism of SULT1A1 is ordered with PAPS and PAP binding to the free enzyme.

In this work, we studied the kinetic mechanism of human SULT1A1. Other SULTs such as human SULT1A3 and rat SULT1A1 (AST-IV) have kinetic properties very similar to those of human SULT1A1. A common kinetic characteristic for almost all cytosolic SULTs is that they all exhibit substrate inhibition. All the SULTs also share the same sulfuryl group donor, PAPS. Human SULT1A1 has been recognized as one of the most important phase II drug-metabolizing enzymes. Understanding the kinetic mechanism of this isoform is important for the understanding of drug metabolism and xenobiotic detoxification.

## REFERENCES


1. Wang, L. Q., and James, M. O. (2006) Inhibition of sulfotransferases by xenobiotics. *Curr. Drug Metab. 7*, 83–104.
2. Nimmagadda, D., Cherala, G., and Ghatta, S. (2006) Cytosolic sulfotransferases. *Indian J. Exp. Biol. 44*, 171–182.
3. Gamage, N., Barnett, A., Hempel, N., Duggleby, R. G., Windmill, K. F., Martin, J. L., and McManus, M. E. (2006) Human sulfotransferases and their role in chemical metabolism. *Toxicol. Sci. 90*, 5–22.
4. Runge-Morris, M., and Kocarek, T. A. (2005) Regulation of sulfotransferases by xenobiotic receptors. *Curr. Drug Metab. 6*, 299–307.
5. Pacifici, G. M. (2004) Inhibition of human liver and duodenum sulfotransferases by drugs and dietary chemicals: A review of the literature. *Int. J. Clin. Pharmacol. Ther. 42*, 488–495.
6. Chapman, E., Best, M. D., Hanson, S. R., and Wong, C. H. (2004) Sulfotransferases: Structure, mechanism, biological activity, inhibition, and synthetic utility. *Angew. Chem., Int. Ed. 43*, 3526–3548.
7. Coughtrie, M. W. (2002) Sulfation through the looking glass-recent advances in sulfotransferase research for the curious. *Pharmacogenomics J. 2*, 297–308.
8. Duffel, M. W., Marshal, A. D., McPhie, P., Sharma, V., and Jakoby, W. B. (2001) Enzymatic aspects of the phenol (aryl) sulfotransferases. *Drug Metab. Rev. 33*, 369–395.
9. Glatt, H., Engelke, C. E., Pabel, U., Teubner, W., Jones, A. L., Coughtrie, M. W., Andrae, U., Falany, C. N., and Meinl, W. (2000) Sulfotransferases: Genetics and role in toxicology. *Toxicol. Lett. 112*−*113*, 341–348.
10. Negishi, M., Pedersen, L. G., Petrotchenko, E., Shevtsov, S., Gorokhov, A., Kakuta, Y., and Pedersen, L. C. (2001) Structure and function of sulfotransferases. *Arch. Biochem. Biophys. 390*, 149–157.
11. Duffel, M. W., and Jakoby, W. B. (1981) On the mechanism of aryl sulfotransferase. *J. Biol. Chem. 256*, 11123–11127.
12. Zhang, H., Varlamova, O., Vargas, F. M., Falany, C. N., Leyh, T. S., and Varmalova, O. (1998) Sulfuryl transfer: The catalytic mechanism of human estrogen sulfotransferase. *J. Biol. Chem. 273*, 10888–10892.
13. Chen, L. J., and Segel, I. H. (1985) Purification and characterization of bile salt sulfotransferase from human liver. *Arch. Biochem. Biophys. 241*, 371–379.
14. Vakiani, E., Luz, J. G., and Buck, J. (1998) Substrate specificity and kinetic mechanism of the insect sulfotransferase, retinol dehydratase. *J. Biol. Chem. 273*, 35381–35387.
15. Singer, S. S., and Bruns, L. (1980) Enzymatic sulfation of steroids. XI. The extensive purification and some properties of hepatic sulfotransferase III from female rats. *Can. J. Biochem. 58*, 660–666.
16. Whittemore, R. M., Pearce, L. B., and Roth, J. A. (1985) Purification and kinetic characterization of a dopamine-sulfating form of phenol sulfotransferase from human brain. *Biochemistry 24*, 2477–2482.
17. Whittemore, R. M., Pearce, L. B., and Roth, J. A. (1986) Purification and kinetic characterization of a phenol-sulfating form of phenol sulfotransferase from human brain. *Arch. Biochem. Biophys. 249*, 464–471.
18. Vargas, F., Frerot, O., Brion, F., Trung Tuong, M. D., Lafitte, A., and Gulat-Marnay, C. (1994) 3′-Phosphoadenosine 5′-phosphosulfate biosynthesis and the sulfation of cholecystokinin by the tyrosylprotein-sulfotransferase in rat brain tissue. *Chem.-Biol. Interact. 92*, 281–291.
19. Frerot, O., and Vargas, F. (1991) Cholecystokinin activation: Evidence for an ordered reaction mechanism for the tyrosyl protein sulfotransferase responsible for the peptide sulfation. *Biochem. Biophys. Res. Commun. 181*, 989–996.
20. Varin, L., and Ibrahim, R. K. (1992) Novel flavonol 3-sulfotransferase. Purification, kinetic properties, and partial amino acid sequence. *J. Biol. Chem. 267*, 1858–1863.
21. Kim, D. H., Kim, H. S., Imamura, L., and Kobashi, K. (1994) Kinetic studies on a sulfotransferase from *Klebsiella* K-36, a rat intestinal bacterium. *Biol. Pharm. Bull. 17*, 543–545.
22. Gorokhov, A., Perera, L., Darden, T. A., Negishi, M., Pedersen, L. C., and Pedersen, L. G. (2000) Heparan sulfate biosynthesis: A theoretical study of the initial sulfation step by N-deacetylase/N-sulfotransferase. *Biophys. J. 79*, 2909–2917.
23. Kakuta, Y., Pedersen, L. G., Carter, C. W., Negishi, M., and Pedersen, L. C. (1997) Crystal structure of estrogen sulphotransferase. *Nat. Struct. Biol. 4*, 904–908.
24. Kakuta, Y., Pedersen, L. C., Chae, K., Song, W. C., Leblanc, D., London, R., Carter, C. W., and Negishi, M. (1998) Mouse steroid sulfotransferases: Substrate specificity and preliminary X-ray crystallographic analysis. *Biochem. Pharmacol. 55*, 313–317.
25. Petrotchenko, E. V., Doerflein, M. E., Kakuta, Y., Pedersen, L. C., and Negishi, M. (1999) Substrate gating confers steroid specificity to estrogen sulfotransferase. *J. Biol. Chem. 274*, 30019–30022.
26. Pedersen, L. C., Petrotchenko, E., Shevtsov, S., and Negishi, M. (2002) Crystal structure of the human estrogen sulfotransferase-PAPS complex: Evidence for catalytic role of Ser137 in the sulfuryl transfer reaction. *J. Biol. Chem. 277*, 17928–17932.

27. Shevtsov, S., Petrotchenko, E. V., Pedersen, L. C., and Negishi, M. (2003) Crystallographic analysis of a hydroxylated polychlorinated biphenyl (OH-PCB) bound to the catalytic estrogen binding site of human estrogen sulfotransferase. *Environ. Health Perspect. 111*, 884–888.
28. Moon, A. F., Edavettal, S. C., Krahn, J. M., Munoz, E. M., Negishi, M., Linhardt, R. J., Liu, J., and Pedersen, L. C. (2004) Structural analysis of the sulfotransferase (3-o-sulfotransferase isoform 3) involved in the biosynthesis of an entry receptor for herpes simplex virus 1. *J. Biol. Chem. 279*, 45185–45193.
29. Edavettal, S. C., Lee, K. A., Negishi, M., Linhardt, R. J., Liu, J., and Pedersen, L. C. (2004) Crystal structure and mutational analysis of heparan sulfate 3-O-sulfotransferase Isoform 1. *J. Biol. Chem. 279*, 25789–25797.
30. Lee, K. A., Fuda, H., Lee, Y. C., Negishi, M., Strott, C. A., and Pedersen, L. C. (2003) Crystal structure of human cholesterol sulfotransferase (SULT2B1b) in the presence of pregnenolone and 3′-phosphoadenosine 5′-phosphate. Rationale for specificity differences between prototypical SULT2A1 and the SULT2BG1 isoforms. *J. Biol. Chem. 278*, 44593–44599.
31. Barnes, S., Waldrop, R., Crenshaw, J., King, R. J., and Taylor, K. B. (1986) Evidence for an ordered reaction mechanism for bile salt 3′-phosphoadenosine-5′-phosphosulfate:sulfotransferase from rhesus monkey liver that catalyzes the sulfation of the hepatotoxin glycolithocholate. *J. Lipid Res. 27*, 1111–1123.
32. Pi, N., Yu, Y., Mougous, J. D., and Leary, J. A. (2004) Observation of a hybrid random ping-pong mechanism of catalysis for NodST: A mass spectrometry approach. *Protein Sci. 13*, 903–912.
33. Kim, D. H., and Kobashi, K. (1991) Kinetic studies on a novel sulfotransferase from Eubacterium A-44, a human intestinal bacterium. *J. Biochem. 109*, 45–48.
34. Lee, N. S., Kim, B. T., Kim, D. H., and Kobashi, K. (1995) Purification and reaction mechanism of arylsulfate sulfotransferase from *Haemophilus* K-12, a mouse intestinal bacterium. *J. Biochem. 118*, 796–801.
35. Kwon, A. R., Yun, H. J., and Choi, E. C. (2001) Kinetic mechanism and identification of the active site tyrosine residue in *Enterobacter amnigenus* arylsulfate sulfotransferase. *Biochem. Biophys. Res. Commun. 285*, 526–529.
36. Pi, N., Hoang, M. B., Gao, H., Mougous, J. D., Bertozzi, C. R., and Leary, J. A. (2005) Kinetic measurements and mechanism determination of Stf0 sulfotransferase using mass spectrometry. *Anal. Biochem. 341*, 94–104.
37. Cook, P. F., and Cleland, W. W. (2007) *Enzyme kinetics and mechanism*, Garland Science, London.
38. Leskovac, V. (2003) *Comprehensive Enzyme Kinetics*, Springer, New York.
39. Purich, D. L., and Allison, R. D. (1980) Isotope exchange methods for elucidating enzymic catalysis. *Methods Enzymol. 64*, 1–46.
40. Chen, G., Battaglia, E., Senay, C., Falany, C. N., and Radominska-Pandya, A. (1999) Photoaffinity labeling probe for the substrate binding site of human phenol sulfotransferase (SULT1A1): 7-Azido-4-methylcoumarin. *Protein Sci. 8*, 2151–2157.
41. Chen, G., Rabjohn, P. A., York, J. L., Wooldridge, C., Zhang, D., Falany, C. N., and Radominska-Pandya, A. (2000) Carboxyl residues in the active site of human phenol sulfotransferase (SULT1A1). *Biochemistry 39*, 16000–16007.
42. Falany, C. N., Krasnykh, V., and Falany, J. L. (1995) Bacterial expression and characterization of a cDNA for human liver estrogen sulfotransferase. *J. Steroid Biochem. Mol. Biol. 52*, 529–539.

BI801211T